Dynamics of Reaction-Diffusion Oscillators in Star and other Networks with Cyclic Symmetries Exhibiting Multiple Clusters

Michael M. Norton[1,*] Nathan Tompkins[1,2,*] Baptiste Blanc,[1] Matthew Carl Cambria,[1]
Jesse Held[1] and Seth Fraden[1,†]

[1]*Physics Department, Brandeis University, Waltham, Massachusetts 02453, USA*
[2]*Physics Department, Wabash College, Crawfordsville, Indiana 47933, USA*

We experimentally and theoretically investigate the dynamics of inhibitory coupled self-driven oscillators on a star network in which a single central hub node is connected to k peripheral arm nodes. The system consists of water-in-oil Belousov-Zhabotinsky ∼100 μm emulsion drops contained in storage wells etched in silicon wafers. We observed three dynamical attractors by varying the number of arms in the star graph and the coupling strength: (i) unlocked, uncorrelated phase shifts between all oscillators; (ii) locked, arm hubs synchronized in phase with a k-dependent phase shift between the arm and central hub; and (iii) center silent, a central hub stopped oscillating and the arm hubs oscillated without synchrony. We compare experiment to theory. For case (ii), we identified a logarithmic dependence of the phase shift on star degree, and were able to discriminate between contributions to the phase shift arising from star topology and oscillator chemistry.

Discrete networks of self-driven oscillators represent a broad class of physical systems [1–11]. Here we focus on an important goal of oscillator network research: to identify how (i) individual oscillator's dynamics, (ii) network topology, and (iii) coupling type conspire to create emergent spatiotemporal patterns in the form of steady phase relationships between oscillators. Addressing this fundamental goal has motivated the development of controlled experimental systems that operate with varying degrees of autonomy [12–20]. In this study we employ a model experimental system consisting of a microfluidically assembled discrete network of Belousov-Zhabotinsky (BZ) chemical oscillators and compare the results with both a discrete reaction-diffusion (RD) network model and phase model.

The theoretical foundation of the BZ reaction is well established enabling near-quantitative modeling of both isolated and coupled oscillators. The novelty of this study arises from our ability to vary the topology and internodal coupling of the network, and to parallelize experiments through microfluidic fabrication techniques [18,19]. We examine inhibitory coupling, which promotes symmetry-breaking phenomena by preferring a π-phase shift between neighbors [16,19,21–25]. We arrange the cells in a network with star topology, consisting of a central hub node connected by k arms to other nodes, as illustrated in Fig. 1, and show how dynamics predictably depart from this simple antiphase synchrony by varying k. Star networks have been considered in theoretical [26] and experimental studies on electronic networks [27], but never in natural systems. Star networks are an important naturally

occurring motif in neural networks that perform cognitive [28–30] and sensorial functions [31], but living neural networks have too many unknown parameters to enable disentangling the roles of oscillator dynamics and network topology on emergent behavior.
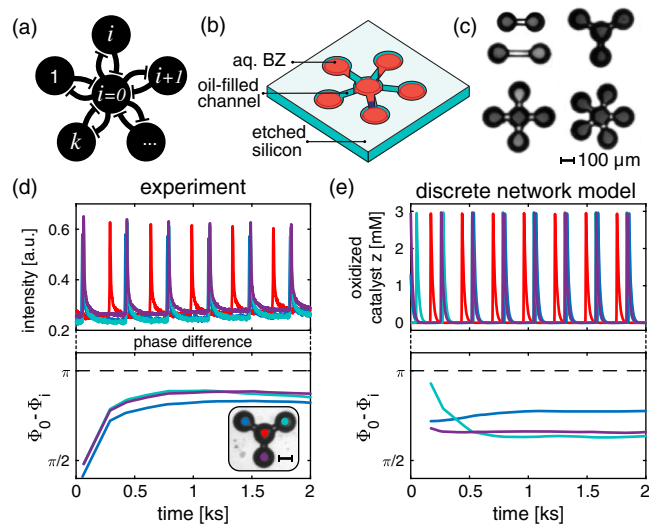

FIG. 1. (a) Schematic of inhibitory-coupled star network of degree k. (b) Schematic of experimental setup: BZ aqueous drops are stored in circular wells etched in a silicon wafer and separated by fluorinated oil. (c) Reflection microscopy images of loaded star networks with different numbers of arms and arm lengths; movies S1–S8 in Ref. [32], (d) and (e) Time trace of droplet intensity and corresponding evolution of arm node phase relative to hub node showing phase locking for experiment (movie S2 [32]) and point model simulation [Eq. (1)].

Notably, our BZ system uses RD processes to produce the oscillator dynamics, star network topology and inhibitory coupling. Thus the dynamics belong to the class of natural physical-chemical phenomena, in contrast to other dynamical systems in which the oscillators, coupling, or both are mediated through electronic hardware [1,2,20,27, 33–35]. Our system therefore demonstrates the potential for creating stand-alone soft materials designed to generate specific self-organized spatiotemporal patterns. Specifically, we seek the engineering principles that control the phase relationship between coupled oscillators. An application of such materials is to make autonomous, soft robots that run purely on chemicals like living organisms, rather than powered by motors and controlled by computers. In this scenario, the BZ network would function as a central pattern generator found in the nervous system of many animals [19].

We probe the dynamical states of the system as a function of internodal coupling strength and star degree, thereby focusing on the impact of physical changes to the star network while taking the BZ chemistry as a known in our experiments and models. We compare observations to two levels of theory: a discrete RD model with Vanag-Epstein [21] chemical dynamics taking place at each node and a phase model constructed from the discrete model that we use to examine the topology dependence of locking angles.

Strikingly, we observe that the locking angle between the cluster formed by synchronized arm nodes and the hub node deviates from perfect antiphase synchrony with a logarithmic dependence on k. The phase model predicts that the prefactor for this dependence depends only on the interaction function and can therefore be numerically derived for any oscillator from a model or an experimentally acquired phase response curve [36]. This result disentangles oscillator and coupling physics from topological effects by compactly showing how each come together to produce topology-dependent phase locking. Since the star graph's cyclic symmetry is responsible for coarsening the system into two clusters, our result will generalize to other networks that can be similarly coarsened by identifying group orbits [1].

Experimental system.—Surfactant stabilized emulsions of 100 micron diameter drops containing the aqueous BZ solution were generated in a fluorinated oil [37]. A drop of the concentrated emulsion was pipetted onto the etched silicon wafer, a cover glass was laid on top and clamped together, thereby squeezing the BZ drops into the etched network and sealing the device. Each wafer contained hundreds of star networks. The design concept was to make a device that was quick to load, intolerant to failure, and reusable. Typically 90% of the networks fail to load correctly. However, 10–20 successes are enough to accumulate statistics. Both the silicon and glass are completely impermeable to all chemical species ensuring that each arm drop only communicates with the hub drop [18].

The cavities containing the BZ drops are connected with channels designed to be too narrow to house drops, but contain oil, and therefore function as diffusive conduits, Fig. 1(b). The BZ reaction oscillates between a reduced and oxidized state of the catalyst. The duration of the oxidized, or activated state, is brief and during this interval a large amount of the inhibitor, bromine, is also generated. The inhibitory coupling between two drops is provided by bromine, which due to its low polarizability readily partitions into the oil [16]. All the chemicals, their concentrations, and conditions for producing the emulsion are described in the Supplemental Material [32].

Theory and model.—In a RD network consisting of $i = 1 \cdots N$ nodes and $m = 1 \cdots M$ species, the dynamics of the concentration c_i^m are governed by

$$\dot{c}_i^m = F_i^m(\mathbf{c}_i) + \sum_{j=1}^{N} \mu_{ij}^m \mathcal{A}_{ij}(c_j^m - c_i^m), \tag{1}$$

where $F_i^m(\mathbf{c}_i)$ models intranodal reactions given by the Vanag-Epstein model of BZ chemistry [21] and the second term captures internodal diffusive transport proportional to the species-dependent coefficient μ_{ij}^m; full expressions are found in the Supplemental Material [32]. This model assumes that all the chemistry occurs at discrete points; i.e., it ignores concentration gradients within a drop. The point approximation is justified because the width of the oxidation front in the BZ reaction is larger than the size of the droplets; thus each reactor oxidizes uniformly.

Modeling the coupling as linearly proportional to the concentration difference between connected nodes is equivalent to ignoring any chemical reactions and accumulation of chemicals in the oil separating drops, which is justified when the interdrop gap is much less than the diffusion length scale $l \sim \sqrt{DT}$, where D is the diffusivity of bromine in oil and the timescale is given by the oscillation period T [16–18]. We consider gaps no greater than 60 μm. With diffusivity $D \sim \mathcal{O}(10^{-9})$ m^2 s^{-1} and oscillation period $T \sim \mathcal{O}(10^2)$ s, the diffusion length scale is $l \sim 300$ μm; thus we are safely in the quasisteady regime. Network connectivity is given by the adjacency matrix $\mathcal{A}$ such that $\mathcal{A}_{ij} = 1$ if i and j are connected and $\mathcal{A}_{ij} = 0$ otherwise. We restrict our attention to the dynamics of Eq. (1) on star graphs with k arm nodes, Fig. 1(a).

We additionally employ the method of phase-reduction to create a further-simplified model of the phase-locked dynamics [32,38,39]. The approach assumes that the state of an isolated multivariable chemical oscillator with limit-cycle dynamics can be fully described with a single phase variable. For weakly coupled oscillators, the slow dynamics of the network, obtained by averaging over one oscillation period, take the form $\dot{\Phi}_i = \omega + \sum_{j=1}^{N} \mathcal{A}_{ij} \mathcal{H}_{ij}(\Phi_{ji})$, where Φ_i and $\dot{\Phi}_i$ are the phase and instantaneous frequency of the ith oscillator, respectively, ω is the frequency of an isolated
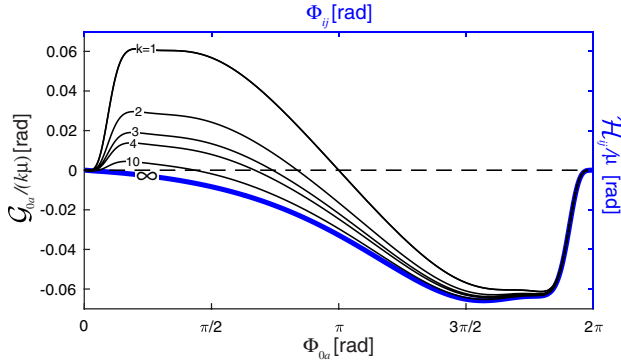
FIG. 2. Interaction function normalized by coupling strength $\mathcal{H}_{ij}/\mu$ (thick blue line) describes how oscillator i's phase changes due to the presence of oscillator j as a function of the phase difference between them $\Phi_{ij} = \Phi_i - \Phi_j$ [40]. $\mathcal{G}/(k\mu)$ describes how the phase *difference* along the k-arm-synchronized manifold $\Phi_1 = \Phi_2 = \cdots = \Phi_k$ evolves as a function of the phase difference between the two clusters, Φ_{0a} (thin lines) [Eq. (2)].
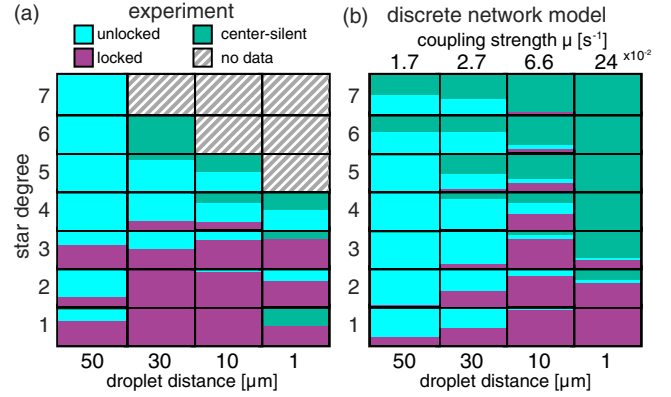

FIG. 3. State diagrams as a function of arm separation (plotted from large to small lengths) and star degree for (a) experiment and (b) point model predictions, Eq. (1), with 7.5% variations in H$^+$ concentration. Hatched region indicates where data were unobtainable due to geometric constraints. Examples of each dynamical state are shown in movies S2–S6.

oscillator (assumed to be identical for all oscillators), $\Phi_{ji} = \Phi_j - \Phi_i$ is the phase difference between two oscillators, and $\mathcal{H}_{ij}$ is a numerically calculated interaction function describing how the instantaneous frequency of oscillator i is changed by the presence of oscillator j, derived from Eq. (1) and shown in Fig. 2 [40]. We model oscillator interactions as occurring entirely through diffusive transport of the inhibitory species bromine; oscillator i is delayed by oscillator j for nearly all Φ_{ij}, with the largest delay occurring just before oscillator i is about to undergo a transition from the reduced to oxidized state. Experimental conditions are chosen to be consistent with the model [16,17].

State diagram.—We observed three dynamical attractors as a function of the number of arms in a star graph and the coupling strength (Fig. 3). The states are (i) unlocked (movie S5), unsynchronized oscillations of all nodes, (ii) locked (movies S2–S4 [32]), arm hubs synchronized in phase with a k-dependent phase shift between the arm and central hub, and (iii) center silent (movie S6 [32]), a nonoscillating, or intermittently oscillating central hub and unsynchronized oscillations of all arm hubs. Using photochemical inhibition, we are also able to change state dynamically by manipulating topology. Shining strong light on a node inhibits oscillation, effectively pruning that node from the network. We induced a transition from center silent to locked in a 5-arm star by shining light on two arms, effectively transforming the network to a 3-arm star while leaving the coupling constant unchanged. We also induced a transition from locked to unlocked by shining light on the hub of a 3-arm star, as shown in movies S7–S8 and Fig. S2 in the Supplemental Material [32].

In Fig. 3, experiment and theory are compared. When the coupling strength is low (large drop separation), the

unlocked state is observed. A network is considered unlocked if a steady-state locking angle is not achieved during the experiment, for theory, we examine a time window commensurate with experiments corresponding to ~20 oscillations. For moderate star degree, as one increases the coupling strength, phase locking is observed. Further increases to the coupling strength result in center-silent dynamics. For large star degree unlocking proceeds directly to center silent. Conversely, as star degree is lowered, the coupling strength range over which phase locking occurs broadens. An analytic expression for the diffusive rate μ [s^{-1}] is presented in the Supplemental Material; we expect μ to be inversely proportional to the drop separation and to the volume of the receiving drop [32].

In order to match the theory-predicted state diagram with the experiment we introduced normally distributed variations of 7.5% in H$^+$, this created a distribution in oscillation periods 223 ± 13 s (~13%); previous observations find 5% variation in intrinsic frequency but also found the need to increase heterogeneity in simulations for good agreement [23]. We ran each parameter combination (k and μ) 20 times, resampling the variation in chemistry and initial conditions each time. We also introduced a coupling strength reduction (fudge) factor $f = 0.15$ to modify the predicted μ. Heterogeneity is needed to both destroy synchrony when coupling is weak [10] and move the transition from locked to center silent to lower k. Phase diagrams showing theoretical predictions without these modifications are shown in the Supplemental Material, Fig. S4 [32].

Variations in parameters are justified because the inner, aqueous phase is composed of two reactant streams; fluctuations in flow rates can therefore produce droplets of varying composition and size. For simplicity, we consider chemical heterogeneity alone. The reduction of the

effective coupling coefficient has been noted previously [23]. These results indicate our idealized model is qualitatively, but not quantitatively, correct and further, that system heterogeneity is an important parameter.

Steady state locking angles and phase model.—The phase interaction function $\mathcal{H}_{ij}$, assuming only bromine transport between oscillators, is nearly completely negative meaning that coupled oscillators mutually delay one another, Fig. 2 (bold curve). This produces a steady state phase shift between two oscillators, at the maximum phase difference of π, Fig. 2 ($k = 1$ curve). Within the phase-locked regime, we experimentally observe that as the number of arms increases, the delay between when the hub and arm nodes oxidize decreases, Figs. 1(d) and 1(e) and Fig. 4(a). We examine this dependence using the numerically constructed phase model.

Since all solutions exhibit arm-locked dynamics, a consequence of the arms forming a single orbit of the star network's graph [1], we examine the dynamics along the
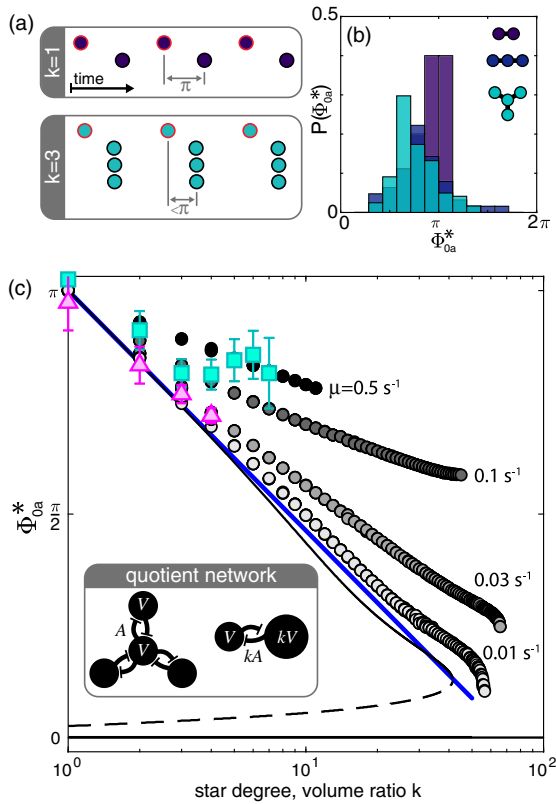

FIG. 4. Locking angle Φ_{0a}^* depends on star degree. (a) Illustration showing how additional arm nodes impact locking angle, (b) histogram of experimental results for $k = 1, 2, 3$ and all coupling strengths, (c) bifurcation diagram comparing phase model (solid black lines are stable fixed points, dashed are unstable), point model [Eq. (1)] with heterogeneity in acid concentration, $\mu = 0.066$ s^{-1} (squares), point model with identical oscillators, $\mu = 0.01$–0.5 s^{-1} (circles), and experiment (triangles). Error bars show standard error. For $\log k \ll 1$, Φ_{0a}^* is given by Eq. (3) (blue line).

arm-synchronized manifold $\Phi_1 = \Phi_2 = \cdots = \Phi_k$ and reduce the system to a single degree of freedom $\Phi_{0a} = \Phi_0 - \Phi_a$ with arm-synchronized cluster a and hub 0. The dynamics of this quotient network are described by

$$\dot{\Phi}_{0a} = k\mathcal{H}_{0a}(-\Phi_{0a}) - \mathcal{H}_{a0}(\Phi_{0a}) = \mathcal{G}(\Phi_{0a}). \quad (2)$$

Examining arm-synchronized dynamics of N oscillators is equivalent to considering a heterogeneous pair: a node containing a single unit of volume V and a large node of volume kV diffusively coupled through a conduit with k times the cross sectional area A of the connections in the original network, inset of Fig. 4(c). This volume difference manifests as an asymmetric coupling constant $\mu_{0a} = k\mu_{a0}$. We report the system dynamics for various k rescaled by the coupling strength and star degree $\mathcal{G}/(k\mu)$ so that as k becomes large the plotted amplitude of the dynamics does not grow as well, Fig. 2.

The system's locking angles are readily given by the fixed points $\mathcal{G}(\Phi_{0a}^*) = 0$ with stability determined by $\mathcal{G}'$ (< 0 stable, > 0 unstable). The results show that for two equally sized nodes, there are four fixed points, two of which are stable $\Phi_{0a}^* = 0, \pi$. However, the basin of attraction associated with $\Phi_{0a}^* = 0$ is so small, it is not visible in Fig. 2(b). In contrast, the basin for $\Phi_{0a}^* = \pi$ is larger and deeper and therefore more accessible and robust against differences in the intrinsic frequencies of the wells, as seen experimentally [37,41].

The phase model predicts that as the volume ratio increases from unity, the hub oscillator is more delayed by the collective action of the arm cluster, shifting Φ_{0a}^*, Fig. 4. As the volume ratio increases, the fixed point continues to move until the volume ratio reaches $1:33.8$ where a saddle-node bifurcation eliminates the attractor, leaving $\Phi_{0a}^* = 0$ as the only attractor, black line in Fig. 4.

These predictions compare favorably to experiment, and the full chemical model without heterogeneity, Fig. 4. In the limit of weak coupling strength, assumed by the creation of the phase model, the locking angle is μ independent. As coupling strength is increased in the point model, predictions diverge with k more rapidly. Additionally, for strong coupling ($\mu = 0.1$–0.5 s^{-1}) the system transitions to center silent while for weaker coupling ($\mu = 0.01$–0.03 s^{-1}) the system instead transitions to in-phase synchrony as predicted by the phase model. Heterogeneity introduced into the model Eq. (1) to reproduce the phase boundaries in Fig. 3 does not change the overall dependence of locking angle on star degree, squares in Fig. 4.

In the limit of weak coupling, $\Phi_{0a}^* - \pi \propto -\log k$, Fig. 4. While physically $k \in \mathbb{N}$ for our system, more generally, k represents the volume ratio between two diffusively coupled oscillators and can take on any positive value. We anticipate logarithmic scaling because the deviation from π should change sign, but not magnitude upon relabeling the quotient graph, which is equivalent to

inverting the volume ratio $\log(k) = -\log(1/k)$. To identify the prefactor, we perform a regular perturbation expansion of the locking angle with $\log(k)$ as the expansion variable, with details provided in the Supplemental Material [32]. The expansion approximates the location of the attractor of Eq. (2) according to the scaling law

$$\Phi_{0a}^* = \pi + \log(k) \frac{1}{2} \mathcal{H}_{0a}(\Phi_{a0}) \left(\frac{d\mathcal{H}_{0a}}{d\Phi_{a0}} \right)^{-1} \Bigg|_{\Phi_{a0}=\pi}, \quad (3)$$

which compares well to the phase model up to $\log k \sim \mathcal{O}(1)$. We emphasize that in the weak-coupling-limit Φ_{0a}^* is μ independent and the comparison between theory and experiment involves zero free parameters. The first term, $\Phi_{0a}^{*(0)} = \pi$, arises from symmetry and is agnostic to oscillator chemistry and network topology. In contrast, the next order correction encodes information specific to both. Information about the chemical reactions enters through the oscillator's phase response curve and coupling to adjacent oscillators through $\mathcal{H}$, while information about network topology enters through $\log k$. We note that while networks of repulsively coupled oscillators have been modeled simply as negatively coupled Kuramoto oscillators $\dot{\Phi}_i = \sum_{j=1}^{N} \mathcal{A}_{ij} \sin (\Phi_j - \Phi_i)$ [42,43], our result shows explicitly that because $\mathcal{H}(\pi) = \sin(\pi) = 0$, sine coupling does not predict the observed topology dependence for branching networks.

Discussion and conclusion.—In this Letter we show how the coupling strength and topology of an inhibitor-coupled BZ RD star network controls transitions between distinct dynamic states. We demonstrate that the high-dimensional RD system of the star network, consisting of $(k+1) \times M$ variables [Eq. (1)], can be reduced to a low-dimensional phase model of k variables and further simplified to a one-dimensional model using the cyclic symmetry of the star graph. Equation (3) explicitly separates topological effects from chemical dynamics and is therefore readily transferable to other oscillator networks. Further, we anticipate that the symmetry-based simplification we employed will generalize to other graphs with orbits originating from cyclic symmetries. While more complex networks generally harbor additional attractors, we speculate that a phase locking attractor with logarithmic dependence on size ratio will exist in cases of unequal cluster size. We expect this to hold even as symmetry-breaking bifurcations break up orbit-generated clusters into smaller synchronized populations. Previous work examining the relationship between dynamics and topology identified conditions for synchronized clusters [1]; here, we obtain a tractable dynamical relationship between clusters of different sizes. Since symmetry-based reductions require identical oscillators it is noteworthy that we observe topology-dependent dynamics to be robust against experimental imperfections. These results demonstrate the utility of model experimental RD systems for both testing theories of network dynamics and providing engineering principles for dynamic soft materials.

[*]These authors contributed equally to this work.
[†]fraden@brandeis.edu

[1] L. M. Pecora, F. Sorrentino, A. M. Hagerstrom, T. E. Murphy, and R. Roy, Cluster synchronization and isolated desynchronization in complex networks with symmetries, Nat. Commun. **5**, 4079 (2014).

[2] F. Sorrentino, L. M. Pecora, A. M. Hagerstrom, T. E. Murphy, and R. Roy, Complete characterization of the stability of cluster synchronization in complex dynamical networks, Sci. Adv. **2**, e1501737 (2016).

[3] N. Kopell and G. Ermentrout, Coupled oscillators and the design of central pattern generators, Math. Biosci. **90**, 87 (1988).

[4] A. W. F. Edwards, Sync-how order emerges from chaos in the universe, nature, and daily life, Math. Intell. **27**, 89 (2005).

[5] M. W. Reimann, M. Nolte, M. Scolamiero, K. Turner, R. Perin, G. Chindemi, P. Dłotko, R. Levi, K. Hess, and H. Markram, Cliques of neurons bound into cavities provide a missing link between structure and function, Front. Comput. Neurosci. **11**, 48 (2017).

[6] Z. Néda, E. Ravasz, T. Vicsek, Y. Brechet, and A. L. Barabási, Physics of the rhythmic applause, Phys. Rev. E **61**, 6987 (2000).

[7] J. Pantaleone, Synchronization of metronomes, Am. J. Phys. **70**, 992 (2002).

[8] F. Dorfler, M. Chertkov, and F. Bullo, Synchronization in complex oscillator networks and smart grids, Proc. Natl. Acad. Sci. U.S.A. **110**, 2005 (2013).

[9] A. Pikovsky, M. Rosenblum, and J. Kurths, in *Cambridge Nonlinear Science Series*, 1st ed. (Cambridge University Press, Cambridge, England, 2003), Vol. 12, p. 432.

[10] S. H. Strogatz, *Nonlinear Dynamics and Chaos* (Westview Press, Cambridge, 2000).

[11] Y. Kuramoto, *Chemical Oscillations, Waves, and Turbulence*, 2nd ed. (Dover, Mineola, 2012).

[12] Y. Jia and I. Z. Kiss, Spontaneously synchronized electrochemical micro-oscillators with nickel electrodissolution, J. Phys. Chem. C **116**, 19290 (2012).

[13] M. Wickramasinghe and I. Z. Kiss, Spatially organized dynamical states in chemical oscillator networks: Synchronization, dynamical differentiation, and chimera patterns, PLoS One **8**, e80586 (2013).

[14] M. Wickramasinghe and I. Z. Kiss, Spatially organized partial synchronization through the chimera mechanism in a network of electrochemical reactions, Phys. Chem. Chem. Phys. **16**, 18360 (2014).

[15] V. Horvath, D. Kutner, J. T. I. Chavis, and I. R. Epstein, Pulse-coupled BZ oscillators with unequal coupling strengths, Phys. Chem. Chem. Phys. **17,** 4664 (2015).

[16] N. Li, J. Delgado, H. O. González-Ochoa, I. R. Epstein, and S. Fraden, Combined excitatory and inhibitory coupling in a 1-D array of Belousov-Zhabotinsky droplets, Phys. Chem. Chem. Phys. **16,** 10965 (2014).

[17] N. Li, N. Tompkins, H. Gonzalez-Ochoa, and S. Fraden, Tunable diffusive lateral inhibition in chemical cells, Eur. Phys. J. E **38,** 18 (2015).

[18] N. Tompkins, M. C. Cambria, A. L. Wang, M. Heymann, and S. Fraden, Creation and perturbation of planar networks of chemical oscillators, Chaos **25,** 064611 (2015).

[19] T. Litschel, M. M. Norton, V. Tserunyan, and S. Fraden, Engineering reaction-diffusion networks with properties of neural tissue, Lab Chip **18,** 714 (2018).

[20] K. A. Blaha, K. Huang, F. Della Rossa, L. Pecora, M. Hossein-Zadeh, and F. Sorrentino, Cluster Synchronization in Multilayer Networks: A Fully Analog Experiment with LC Oscillators with Physically Dissimilar Coupling, Phys. Rev. Lett. **122,** 014101 (2019).

[21] V. K. Vanag and I. R. Epstein, A model for jumping and bubble waves in the Belousov-Zhabotinsky-aerosol OT system, J. Chem. Phys. **131,** 104512 (2009).

[22] V. K. Vanag and I. R. Epstein, Excitatory and inhibitory coupling in a one-dimensional array of Belousov-Zhabotinsky micro-oscillators: Theory, Phys. Rev. E **84,** 066209 (2011).

[23] N. Tompkins, N. Li, C. Girabawe, M. Heymann, G. B. Ermentrout, I. R. Epstein, and S. Fraden, Testing Turing's theory of morphogenesis in chemical cells, Proc. Natl. Acad. Sci. U.S.A. **111,** 4397 (2014).

[24] J. Guzowski, K. Gizynski, J. Gorecki, and P. Garstecki, Microfluidic platform for reproducible self-assembly of chemically communicating droplet networks with predesigned number and type of the communicating compartments, Lab Chip **16,** 764 (2016).

[25] K. Torbensen, F. Rossi, S. Ristori, and A. Abou-Hassan, Chemical communication and dynamics of droplet emulsions in networks of Belousov-Zhabotinsky micro-oscillators produced by microfluidics, Lab Chip **17,** 1179 (2017).

[26] L. M. Pecora and T. L. Carroll, Master Stability Functions for Synchronized Coupled Systems, Phys. Rev. Lett. **80,** 2109 (1998).

[27] A. Bergner, M. Frasca, G. Sciuto, A. Buscarino, E. J. Ngamga, L. Fortuna, and J. Kurths, Remote synchronization in star networks, Phys. Rev. E **85,** 026208 (2012).

[28] P. Bonifazi, M. Goldin, M. A. Picardo, I. Jorquera, A. Cattani, G. Bianconi, A. Represa, Y. Ben-Ari, and R. Cossart, GABAergic hub neurons orchestrate synchrony in developing hippocampal networks, Science **326,** 1419 (2009).

[29] M. P. van den Heuvel and O. Sporns, Network hubs in the human brain, Trends Cognit. Sci. **17,** 683 (2013).

[30] M. A. Bertolero, B. T. T. Yeo, D. S. Bassett, and M. D'Esposito, A mechanistic model of connector hubs, modularity and cognition, Nat. Human Behav. **2,** 765 (2018).

[31] A. Khaledi-Nasab, J. A. Kromer, L. Schimansky-Geier, and A. B. Neiman, Variability of collective dynamics in random tree networks of strongly coupled stochastic excitable elements, Phys. Rev. E **98,** 052303 (2018).

[32] See Supplemental Material at http://link.aps.org/supplemental/10.1103/PhysRevLett.123.148301 for movies and additional details on experimental preparation and numerical simulations.

[33] J. Miyazaki and S. Kinoshita, Method for determining a coupling function in coupled oscillators with application to Belousov-Zhabotinsky oscillators, Phys. Rev. E **74,** 056209 (2006).

[34] I. Z. Kiss, Z. Kazsu, and V. Gaspar, Tracking unstable steady states and periodic orbits of oscillatory and chaotic electrochemical systems using delayed feedback control, Chaos **16,** 033109 (2006).

[35] J. F. Totz, J. Rode, M. R. Tinsley, K. Showalter, and H. Engel, Spiral wave chimera states in large populations of coupled chemical oscillators, Nat. Phys. **14,** 282 (2018).

[36] T. Stankovski, T. Pereira, P. V. E. McClintock, and A. Stefanovska, Coupling functions: Universal insights into dynamical interaction mechanisms, Rev. Mod. Phys. **89,** 045001 (2017).

[37] J. Delgado, N. Li, M. Leda, H. O. González-Ochoa, S. Fraden, and I. R. Epstein, Coupled oscillations in a 1D emulsion of Belousov-Zhabotinsky droplets, Soft Matter **7,** 3155 (2011).

[38] E. Izhikevich, in *Dynamical Systems in Neuroscience: The Geometry of Excitability and Bursting* (MIT Press, Cambridge, 2007), 1st ed..

[39] B. Monga, D. Wilson, T. Matchen, and J. Moehlis, Phase reduction and phase-based optimal control for biological systems: A tutorial, Biol. Cybern. **113,** 11 (2019).

[40] We note that by convention [38] $\mathcal{H}_{ij}$ is defined to be a function of $\Phi_j - \Phi_i$; however, in Fig. 2 we plot as a function of $\Phi_i - \Phi_j$ to compare to $\mathcal{G}$. This change in variables mirrors the function about $\Phi = \pi$, changing the sign of the slope $d\mathcal{H}_{ij}/d\Phi_{ji} = -d\mathcal{H}_{ij}/d\Phi_{ij}$.

[41] M. Toiya, H. O. González-Ochoa, V. K. Vanag, S. Fraden, and I. R. Epstein, Synchronization of chemical micro-oscillators, J. Phys. Chem. Lett. **1,** 1241 (2010).

[42] J. A. Acebrón, L. L. Bonilla, C. J. Vicente, F. Ritort, and R. Spigler, The Kuramoto model: A simple paradigm for synchronization phenomena, Rev. Mod. Phys. **77,** 137 (2005).

[43] M. Giver, Z. Jabeen, and B. Chakraborty, Phase and frequency entrainment in locally coupled phase oscillators with repulsive interactions, Phys. Rev. E **83,** 046206 (2011).